Proc. Natl. Acad. Sci. USA
Vol. 89, pp. 2017–2021, March 1992
Biochemistry

Early hydrogen-bonding events in the folding reaction of ubiquitin

(protein folding/kinetics/nuclear magnetic resonance/hydrogen exchange/rapid mixing)

MARTHA S. BRIGGS* AND HEINRICH RODER

Department of Biochemistry and Biophysics, University of Pennsylvania, Philadelphia, PA 19104-6059; and Institute for Cancer Research, Fox Chase Cancer Center, 7701 Burholme Avenue, Philadelphia, PA 19111

Communicated by Robert L. Baldwin, December 2, 1991

ABSTRACT **The formation of hydrogen-bonded structure in the folding reaction of ubiquitin, a small cytoplasmic protein with an extended β-sheet and an α-helix surrounding a pronounced hydrophobic core, has been investigated by hydrogen–deuterium exchange labeling in conjunction with rapid mixing methods and two-dimensional NMR analysis. The time course of protection from exchange has been measured for 26 backbone amide protons that form stable hydrogen bonds upon refolding and exchange slowly under native conditions. Amide protons in the β-sheet and the α-helix, as well as protons involved in hydrogen bonds at the helix/sheet interface, become 80% protected in an initial 8-ms folding phase, indicating that the two elements of secondary structure form and associate in a common cooperative folding event. Somewhat slower protection rates for residues 59, 61, and 69 provide evidence for the subsequent stabilization of a surface loop. Most probes also exhibit two minor phases with time constants of about 100 ms and 10 s. Only two of the observed residues, Gln-41 and Arg-42, display significant slow folding phases, with amplitudes of 37% and 22%, respectively, which can be attributed to native-like folding intermediates containing cis peptide bonds for Pro-37 and/or Pro-38. Compared with other proteins studied by pulse labeling, including cytochrome *c*, ribonuclease, and barnase, the initial formation of hydrogen-bonded structure in ubiquitin occurs at a more rapid rate and slow-folding species are less prominent.**

A central goal of experimental protein folding studies is to obtain structural and kinetic information on intermediate states between the disordered polypeptide chain of a denatured protein and the folded structure of a native protein. The existence of protein folding pathways with well-defined intermediates is now widely accepted (1, 2), but we know little about the nature of folding intermediates in precise structural terms. Because of the cooperative nature of folding–unfolding transitions, partially folded forms are rarely observed at equilibrium, and kinetic intermediates tend to be too short-lived for the direct application of high-resolution structural tools such as two-dimensional NMR.

Our approach to this problem makes use of pulsed hydrogen–deuterium (H–D) exchange in conjunction with rapid mixing methods and two-dimensional NMR analysis (3, 4). In a typical pulse-labeling experiment, the protein is initially unfolded in a D_2O denaturant solution so that the labile backbone amide protons (NH) are replaced by deuterons (ND). Refolding, initiated by rapid dilution of the denaturant, is allowed to proceed in D_2O (or in H_2O at mildly acidic pH, where NH exchange is slow) for various times before the partially refolded protein is briefly exposed to H_2O at basic pH. Amide hydrogens that are still exposed at this time become protonated during the labeling pulse, while those that are already protected from exchange (e.g., by forming hydrogen bonds) remain deuterated. After the labeling pulse, the protein is allowed to refold at low pH, where exchange is slow and many amide probes become trapped within the refolded protein. The pattern of H and D labels imprinted by the pulse can then be analyzed by two-dimensional ^1H NMR for all those amide probes that exchange slowly under native conditions. In a series of pulse-labeling experiments at different refolding times, one can thus observe the time course of structure formation in terms of the protection of individual amide probes as they become involved in hydrogen-bonded structure during refolding.

The strategy of combining H–D exchange labeling with rapid mixing methods and NMR analysis was initially applied to bovine pancreatic trypsin inhibitor (5) by using a competition method and one-dimensional NMR. More recent folding studies on cytochrome *c* (3), ribonuclease A (4), and barnase (6) made use of the more powerful pulse labeling two-dimensional NMR approach. In the work on cytochrome *c*, amide protons in two helical segments near each end of the polypeptide chain were found to be protected in a common early folding step (20 ms), indicating that the two helices form and associate before stable hydrogen-bonded structure is formed in other parts of the molecule (3, 7). Similar studies on ribonuclease A showed that NH sites in the β-sheet are protected at an early stage compared with the slow folding phases detected by a change in tyrosine absorbance, suggesting that the β-sheet is formed before the hydrophobic core is fully developed (4, 8). Similarly, for barnase it was shown that amide probes in the β-sheet and some helical sites are protected prior to tertiary probes that follow the fluorescence-detected folding kinetics. In each case, native-like elements of secondary structure were found to be formed at an early stage of folding. This is consistent with kinetic circular dichroism results, which indicate very rapid formation of secondary structure for several proteins (9). Furthermore, the helix association event observed for cytochrome *c* shows that the formation of secondary structure is accompanied by some stabilizing tertiary interactions. To assess the generality of these results, it is necessary to extend these studies to other protein systems.

Ubiquitin is a particularly good model protein for folding studies, as well as a very interesting protein from a functional point of view (10, 11). It consists of a single polypeptide chain of 76 amino acids without any cysteines, metals, or extrinsic cofactors. The x-ray coordinates refined at 1.8-Å resolution (12) reveal a globular structure with a pronounced hydrophobic core surrounded by regular secondary structure, including five strands of β-sheet and four turns of α-helix (see Fig. 4). This preponderance of hydrogen-bonded secondary structure makes ubiquitin a good candidate for pulse labeling studies, since only protons that exchange slowly in the native protein can be used as probes for structure formation (3, 4).

The publication costs of this article were defrayed in part by page charge payment. This article must therefore be hereby marked "*advertisement*" in accordance with 18 U.S.C. §1734 solely to indicate this fact.

Abbreviations: Gdn·HCl, guanidine hydrochloride; COSY, two-dimensional *J*-correlated NMR spectroscopy.

*Present address: School of Chemistry and Biochemistry, Georgia Institute of Technology, Atlanta, GA 30332-0400.

Ubiquitin is also very well suited for NMR studies because of its small size, extreme stability, and excellent water solubility; complete ^{1}H NMR resonance assignments have been published (13, 14).

MATERIALS AND METHODS

Materials. Ubiquitin was purchased from Sigma and used without further purification. Guanidine hydrochloride (Gdn·HCl), ultrapure grade, was obtained from Schwartz/Mann. Deuterated Gdn·HCl was prepared by repeated lyophilization of Gdn·HCl from D_2O (99.9%, Isotech, Miamisburg, OH). Gdn·HCl concentrations were calculated from the refractive index of saturated stock solutions (15).

NMR Spectroscopy. ^{1}H NMR spectra at 500 MHz were recorded at 25°C on a Bruker AM 500 spectrometer. For one-dimensional ^{1}H NMR spectra, 256 transients of 4096 complex data points covering a spectral width of 6024 Hz were acquired. Resonance integration was performed on the Aspect 3000 computer of the spectrometer.

For two-dimensional *J*-correlated NMR spectroscopy (COSY) (absolute magnitude mode), 96 transients of 1024 complex data points each, covering a spectral width of 6024 Hz, were recorded for each of 400 t_1 increments (0–66 ms). The data were processed on a MicroVAX computer, using the program FTNMR, kindly provided by Dennis Hare (Hare Research, Woodinville, WA). Unshifted sine multiplication and a 1-Hz line broadening were applied in both dimensions before Fourier transformation. The final digital resolution was 5.9 Hz per point in both dimensions. Cross-peak intensities were measured by volume integration, using a radius of two points.

Rapid Mixing Procedures. For the preparation of ubiquitin samples by the pulse-labeling method, we followed previously developed procedures (3, 16). Rapid mixing experiments were performed at 25°C on a preparative quenched-flow apparatus (QFM-5, from Bio-Logic, Echirolles, France) equipped with three Berger-type mixing chambers and two variable delay lines. Ubiquitin was initially dissolved at 4.5–6 mM in D_2O containing 6 M Gdn·HCl, and the pD (uncorrected pH electrode reading) was adjusted to 3.5 by adding small amounts of dilute DCl or NaOD. The solution was incubated at 25°C for at least 30 min to allow for complete H–D exchange of the amide protons. Refolding was initiated by rapid 6-fold dilution with 50 mM acetic acid at pH 5.5 in H_2O (or D_2O for folding times >1 s). The final pH of the mixture was 5.0, as determined in a separate control. The resulting Gdn·HCl concentration, 1.0 M, is well below the refolding transition (see Fig. 1). After the desired refolding time, the labeling pulse was initiated by mixing the protein with an equal volume of 100 mM glycine in H_2O at pH 9.75, to give a final pH of 9.4. Under these conditions, the exchange time constant for freely accessible amide protons is about 0.5 ms (17–19). The pulse was terminated after 31 ms by mixing with an equal volume of 500 mM acetic acid at pH 2.6, yielding a final pH of 3.4. The samples were concentrated at 4°C by ultrafiltration, washed three times with 1.7 ml of 50 mM deuterated acetic acid in D_2O, pD 3.5. The final ubiquitin concentration was 1–3 mM. Before NMR analysis, each sample was incubated for 30 min at 45°C, in order to exchange some partially labeled amide sites.

For pulse labeling experiments at folding times from 3.4 to 100 ms (delay between the first two mixers), the quench-flow apparatus was operated in continuous-flow mode, whereas an interrupted-flow protocol with a 200-μl delay line was used for longer folding times. The shortest aging time (3.4 ms) was achieved by using flow rates up to 6 ml/s and an aging volume of 20 μl between the first two mixers. Quantitation of the mixing time is difficult for such quench-flow experiments, but stopped-flow experiments under similar conditions on an instrument with the same mixer design indicated that complete mixing was achieved in <2 ms.

RESULTS AND DISCUSSION

Equilibrium Studies. Previous physical studies indicated that ubiquitin is stable under a variety of extreme conditions of temperature and pH. At room temperature and neutral pH, it cannot be fully denatured, even in concentrated Gdn·HCl solution (20). However, under acidic conditions, 6 M Gdn·HCl disrupts all hydrogen-bonded structure in ubiquitin. The single histidine in ubiquitin, His-68, provides a convenient probe for NMR observation of its unfolding–refolding equilibrium (Fig. 1 *Inset*). Separate resonances are observed for the His-68 C_2H in folded and unfolded molecules, indicating that the transition between the two forms is slow on the NMR time scale. The fractions of folded and unfolded protein were calculated from the areas of the corresponding histidine C_2H resonances. The denaturant-induced unfolding transition at pD 3.5 occurs between 2.5 and 5 M Gdn·HCl, with a midpoint at 3.7 M (Fig. 1). When Gdn·HCl concentration is plotted vs. unfolding free energy, $\Delta G°$, a straight line results with a slope of 1.35 kcal·mol^{-1}·M^{-1}. Extrapolation to 0 M Gdn·HCl by use of the linear model (15, 21) yields $\Delta G° = 5.0$ kcal/mol. The transition is fully reversible, as indicated by the observation of identical NMR spectra before the addition of Gdn·HCl and after its removal by gel filtration. Amide proton exchange rates measured for ubiquitin in 6 M Gdn·HCl at pH 3.5 (data not shown) are in agreement with the rates expected for an unstructured polypeptide (17–19), ruling out any residual hydrogen-bonded structure. In addition, the ^{1}H NMR spectrum under these denaturing conditions lacks any features indicative of stable folded structure, such as chemical shift dispersion for chemically identical protons.

Pulse Labeling. To measure the time course of folding, ubiquitin samples were prepared at different refolding times from 3.4 ms to 20 s by using the mixing procedures described

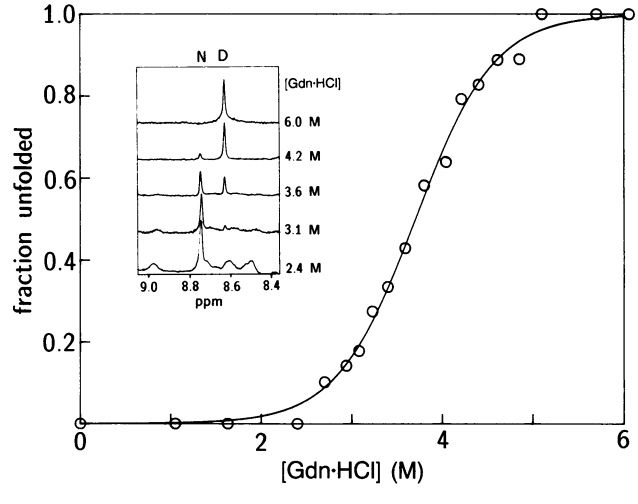

FIG. 1. Reversible unfolding transition of ubiquitin induced by Gdn·HCl, as shown by using the C_2H resonance of His-68 in the ^{1}H NMR spectrum as a conformational probe. Samples contained 2.75 mM ubiquitin, 45 mM deuterated acetic acid, and 0–6.1 M Gdn·HCl in D_2O at pD 3.5 (uncorrected). ^{1}H NMR spectra at 500 MHz (*Inset*) were recorded at 25°C (N, native; D, denatured). The broad lines in the spectrum at 2.4 M Gdn·HCl are due to residual unexchanged amide protons. The fraction of unfolded molecules at each Gdn·HCl concentration was calculated from the area of the His C_2H resonance in the unfolded protein (8.63 ppm), divided by the total C_2H resonance area in the native form (8.75 ppm) and the unfolded form. The curve was calculated based on a two-state model for the folding–unfolding equilibrium, assuming linear dependence of $\Delta G°$ on denaturant concentration (see text).

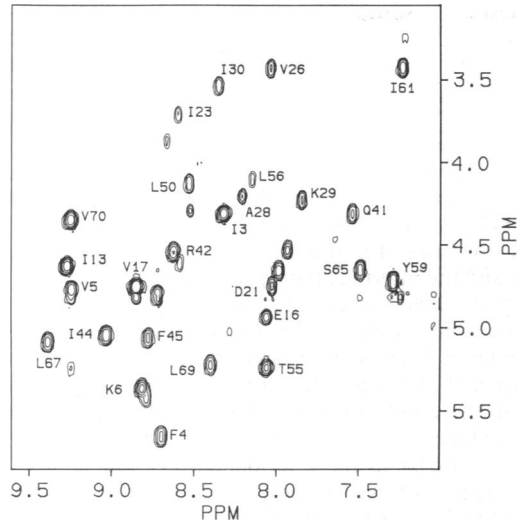

FIG. 2. Fingerprint region of a COSY spectrum containing backbone NH–C_αH cross peaks, recorded at 25°C from a fresh solution of ubiquitin in D_2O with 50 mM deuterated acetic acid, pD 3.5. Cross-peak assignments were derived from ref. 13, by taking into account minor chemical-shift changes due to differences in sample conditions. In a few ambiguous cases, assignments were verified by tracing spin systems in the aliphatic region of the COSY spectrum.

above. The two-dimensional NMR analysis is illustrated in Fig. 2 with a fully protonated control sample consisting of a fresh ubiquitin solution in D_2O buffer at pD 3.5. The fingerprint region of the COSY spectrum contains 26 resolved NH–C_αH cross peaks associated with slowly exchanging amide protons, which are labeled according to the published assignments (13, 14). The spectra recorded on pulse-labeled samples were very similar, except for the intensity of the NH–C_αH cross peaks, which decreased toward longer folding times. Very small cross peaks were observed at the longest folding time used (20 s), indicating that the amide probes were almost completely protected within the refolded protein and remained deuterated.

The two-dimensional NMR data were quantitated by measuring volumes for all resolved NH–C_αH cross peaks. To allow comparison of the spectra from different samples, the average volume of three cross peaks between nonlabile protons (data not shown) was used as an internal intensity standard. The proton occupancy (fractional protonation) at individual amide NH sites was then obtained by dividing a given cross-peak volume by the volume of the same cross peak in the fully protonated control sample, after correction for the fraction of D_2O present during labeling (8.3%). Fig. 3 shows plots of proton occupancy for several backbone amides vs. refolding time on a logarithmic scale. The ribbon diagram shown in Fig. 4 helps to locate these probes in the native ubiquitin structure.

Kinetic and Structural Patterns. Our interpretation of the pulse-labeling results is based on the assumption that protection from NH exchange reflects hydrogen-bond formation. In native proteins, slowly exchanging amide protons are in most cases involved in stable hydrogen-bonded structure, and rapid exchange rates generally indicate lack of intramolecular hydrogen bonding and exposure to solvent (23). However, it is important to keep in mind that hydrogen-bond acceptors cannot be directly identified by NH exchange methods alone. Nevertheless, the structural patterns of protection observed for several stable and transient folding intermediates suggest native-like conformation (24), and we are assuming that hydrogen-bond donor–acceptor pairs are those found in the fully folded protein.

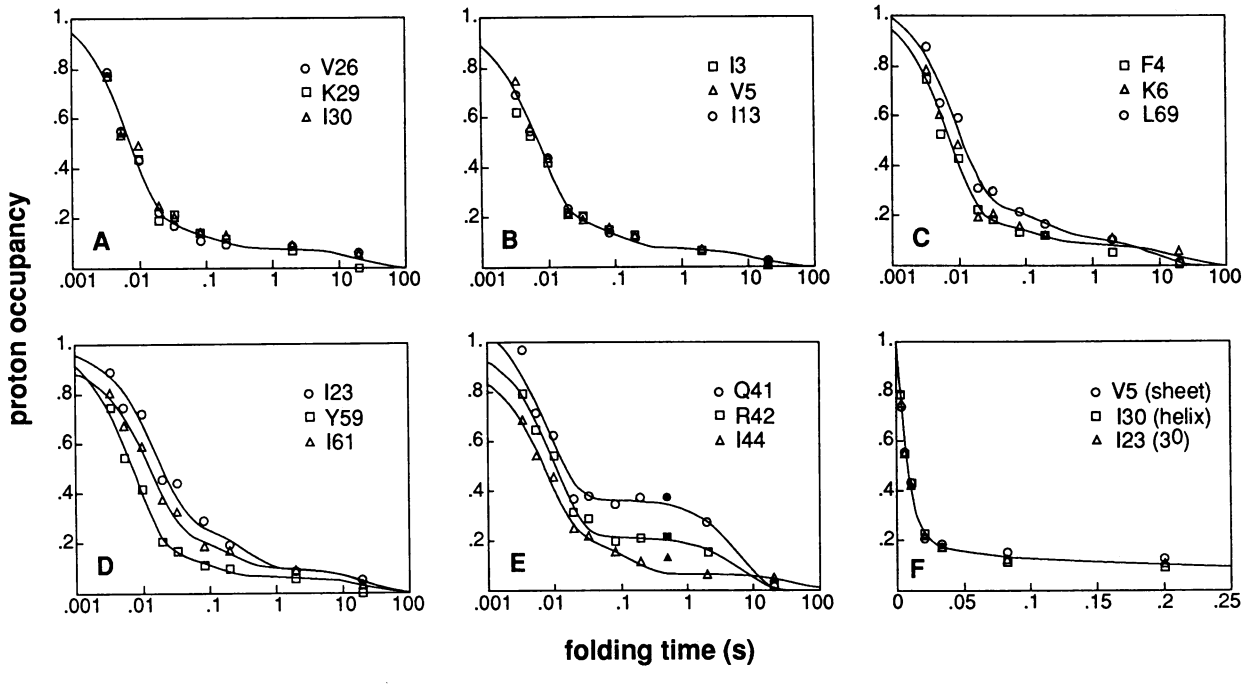

FIG. 3. Time course of protection from D–H exchange for representative ubiquitin backbone amide sites. Proton occupancy is plotted versus refolding time on a logarithmic scale (1 ms to 100 s), except for *F*, which has a linear time scale (0–250 ms). Protons were chosen from the following structural regions of ubiquitin (see Fig. 4): Hydrogen-bonded amide protons in the α-helix (*A*); hydrogen bonds between the two antiparallel strands of the β-sheet near the N terminus (*B*); hydrogen bonds connecting the two parallel β-strands (*C*); protons involved in irregular hydrogen bonds between distant parts of the chain (*D*); a loop region following Pro-37 and Pro-38, leading into an antiparallel β-strand (*E*). The simultaneous protection of protons in diverse structure elements is illustrated in *F*, in which the time course of protection is plotted on a linear time scale for amide probes from the α-helix (Ile-30), the β-sheet (Val-5), and the helix/sheet interface (Ile-23). The curves represent fits of two (for Gln-41 and Arg-42) or three (all other residues) exponential phases (see text). A 31-ms proton labeling pulse at pH 9.4 was used for all experiments, except for the filled symbols in *E*, which were measured at a pulse pH of 10.

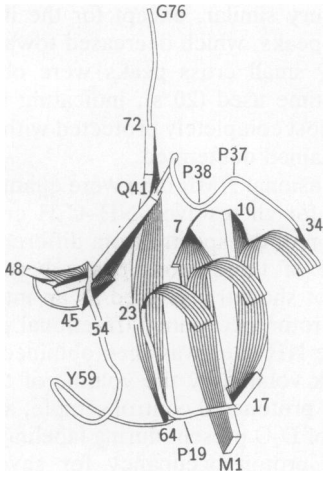

FIG. 4. Ribbon diagram of the ubiquitin backbone, based on the x-ray coordinates of Vijay-Kumar *et al.* (12). The diagram was generated using the Priestle–Callahan ribbon drawing program (22).

It is apparent from Fig. 3 that ubiquitin folds very rapidly. Most amide probes become >80% protected within the first 20 ms of refolding, followed by two minor phases. Kinetic analysis by nonlinear least-squares procedures (solid curves) shows that the data for most probes can be fit by a sum of three decaying exponentials with time constants τ (and amplitudes) of about 8 ms (80%), 100 ms (12%), and 10 s (8%). Two probes, Gln-41 and Arg-42, exhibit a similar fast phase and a more pronounced slow phase, and one amide proton (Ile-61) shows a somewhat slower initial protection phase followed by a minor slow phase. The initial amplitude, obtained by extrapolation to $t = 0$, lies near 1.0 (±5%) for all observed amide probes (e.g., Fig. 3*F*), indicating that the kinetics of protection is fully accounted for by the measurements and that there are no apparent mixing artifacts. Any rapid protection phases occurring in the dead time of the mixing experiment would result in lower proton occupancies for the early time points and initial amplitudes of <1.0.

Fig. 3*A* shows examples of amide protons that form hydrogen bonds within the α-helix of the native ubiquitin structure (*cf.* Fig. 4). The extreme cooperativity of helix formation, indicated by the superposition of data points from different probes, is notable. The time course of protection for protons involved in hydrogen bonds that bridge the N-terminal pair of antiparallel β-strands (Ile-3, Val-5, and Ile-13) is shown in Fig. 3*B*. The kinetics of protection is again virtually identical for these structurally related probes, indicating that formation of the β-sheet is a highly cooperative event. Protons involved in hydrogen bonds that span the single pair of parallel strands show somewhat larger differences in folding kinetics (Fig. 3*C*). The difference in the major phase time constants between the most rapidly protected proton (Phe-4, τ = 6 ms) and the most slowly protected proton (Leu-69, τ = 12 ms) is 2-fold, although, on average, these protons are protected at about the same rate as those in the α-helix and the remainder of the β-sheet. Hydrogen-bonded amide protons in some reverse turns (data not shown) show folding kinetics very similar to that of the sheet and helix.

The pulse-labeling results for a typical helical probe (Ile-30) and one of the β-sheet protons (Val-5) are compared in Fig. 3*F*, on a linear time scale. The observation of nearly identical behavior for amide protons in diverse structural elements (α-helix, parallel and antiparallel β-sheet) implies that the core of the protein is formed in a single cooperative step. In support of this, some "tertiary" hydrogen bonds (hydrogen bonds in regions of irregular structure between residues that are distant in the primary sequence), like the hydrogen bond from the amide proton of Ile-23 to the carbonyl of Arg-54 (Fig. 3 *D* and *F*) and that from the Leu-56 amide proton to the backbone carbonyl of Asp-21 (data not shown), exhibit a major protection phase with the same time constant as most of the secondary structure probes. The strategic location of these hydrogen bonds between the helix and sheet makes them key indicators of the proximity of the major elements of secondary structure, and of the probable formation of the hydrophobic core between them.

Thus, the core of ubiquitin, composed of the α-helix and β-sheet and the interface between them, is formed in a major cooperative folding event. The sheet and helix protons are protected at nearly identical rates, indicating cooperativity in the formation both of the individual elements of secondary structure and of the interfacial region. The rapid protection rates for the amide protons of Ile-23 and Leu-56 provide direct evidence for early association of the sheet and the helix. In a similar fashion, association of the N- and C-terminal α-helices of cytochrome *c* at an early stage of folding appears to be required for helix stabilization (3).

Not all amide probes exhibit the same kinetics of protection. For example, the initial protection phase for Ile-61 (Fig. 3*D*) is significantly slower (τ = 15 ms) than that of the majority of the α-helix and β-sheet protons (τ = 8 ms), with similar amplitudes for the major phase (70–80%). Somewhat retarded protection is also observed for two other probes, Tyr-59 (Fig. 3*D*) and Leu-69 (data not shown). In the native ubiquitin structure (see Fig. 4), these amide protons and their hydrogen-bonding partners are part of a peripheral loop region containing several irregular hydrogen bonds. This surface region appears to be formed at a somewhat slower rate in a sequential step following the formation of the central sheet/helix domain.

Minor Folding Events. All of the amide probes observed in this study exhibit at least two exponential protection phases, which is indicative of a heterogeneous mixture with two or more populations of molecules folding along parallel pathways. Evidence for multiple parallel pathways has been obtained for ribonuclease A (8) and cytochrome *c* (7), based on pulse-labeling experiments involving systematic variation of the labeling conditions. For ubiquitin, all of the observed amide probes display a slow phase with an amplitude of at least 9%, which is consistent with a minor population of molecules that remain unfolded (in terms of NH protection) out to long refolding times. The amide protons of Gln-41 and Arg-42 exhibit more pronounced slow protection phases, with relative amplitudes of 37% and 22%, respectively. Thus, the folding reaction appears to be heterogeneous, with some molecules acquiring native-like hydrogen-bonded structure on the 10-ms time scale, while others lack one or more native hydrogen bonds out to about 10 s. The heterogeneous nature of folding was confirmed by parallel experiments in which labeling was performed at pH 10 instead of pH 9.4, but with otherwise identical conditions. The slow phase is evident at both pH values, with essentially the same amplitude, as indicated by the filled symbols in Fig. 3*E*. This insensitivity to labeling conditions (pulse pH or time) is characteristic of a heterogeneous mixture of molecules that are either fully protected or fully labeled during the pulse (7, 8).

Interestingly, the amide protons with the most pronounced slow folding phases (Gln-41 and Arg-42) are adjacent to two proline residues (Pro-37 and Pro-38), with a hydrogen bond between the NH of Gln-41 and the carbonyl oxygen of Pro-38, suggesting that cis–trans isomerization of proline peptide bonds may be responsible for their slow folding phases. The involvement of proline isomerization in the kinetics of protein folding has been studied extensively for many proteins (reviewed in refs. 1 and 25). Ubiquitin contains three proline residues, all of which are preceded by trans peptide bonds in the native structure (12). However, each has an equilibrium

distribution of cis and trans isomers in the unfolded polypeptide, typically with about 80% trans and 20% cis forms (26). Our pulse labeling results can be rationalized in terms of a simple model involving cis and trans isomers for all three proline residues. The calculations are based on three assumptions. (*i*) If Pro-19 is preceded by a cis peptide bond, the folding of the entire molecule is affected, and all backbone amide protons remain unprotected until cis–trans isomerization occurs [an essential proline residue according to the classification of Levitt (27)]. Since our data show that most of the observed protons have, on average, about 9% slow phase, we estimate that the equilibrium distribution of cis and trans isomers for Pro-19 is about 9% cis and 91% trans. (*ii*) The amide proton of Arg-42 is protected from exchange only if Pro-37 is preceded by a trans peptide bond. Thus, the 22% slow phase of Arg-42 is due to a cis peptide bond at either Pro-19 or Pro-37, or both. (*iii*) If either Pro-37 or Pro-38 is preceded by a cis peptide bond, we assume that Gln-41 is unable to form a hydrogen bond to Pro-38. In this case, the 37% slow phase of Gln-41 is caused by a cis peptide bond at any of the three proline residues. With these assumptions, we estimate the following equilibrium distributions of cis and trans isomers: 9% cis, 91% trans for Pro-19; 14% cis, 86% trans for Pro-37; 19% cis, 81% trans for Pro-38.

The assumptions above imply that the loop including residues 37–42 is structurally decoupled from the remainder of the protein, since major disruptions in the local structure (cis peptide bonds at residues 37 and/or 38) do not propagate into other parts of the molecule. Pro-19, on the other hand, occupies a more strategic position at the junction between the second strand of the β-sheet and the beginning of the α-helix. The presence of a cis peptide bond at this position appears to inhibit the formation of stable hydrogen-bonded structure in all regions of the protein, supporting the idea that association of elements of secondary structure is necessary for structural stabilization.

It is interesting that the estimated trans/cis equilibrium constant for Pro-19 is about 10, while for Pro-37 and Pro-38 it is only 4–6. Since the trans/cis equilibrium constant in an unfolded polypeptide varies with sequence (26), this raises the question of how the evolution of the peptide sequence surrounding proline residues has been affected by the necessity for efficient folding.

Summary and Conclusions. Ubiquitin folds extremely rapidly and cooperatively, with the majority of protons protected against labeling in a major kinetic phase on the 10-ms time scale. Association of elements of secondary structure appears to be important in driving this early folding event. A region of irregular structure including Tyr-59, Ile-61, and Leu-69 folds somewhat more slowly. In addition, there are indications for minor slow-folding species due to unfolded molecules containing one or more proline residues with cis peptide bonds. The slow protection phases for Gln-41 and Arg-42 appear to be due to local structural perturbations caused by the presence of cis peptide bonds adjacent to Pro-37 and/or Pro-38 in otherwise native-like intermediates. A minor slow protection phase observed for all amide probes can be attributed to the remaining proline residue at position 19, where cis–trans isomerization appears to have a more global effect.

The speed of ubiquitin folding may bear on some of its functions *in vivo*. Ubiquitin is synthesized initially as a fusion protein, carrying as a C-terminal extension one of two ribosomal proteins (28, 29). The ubiquitin fusion appears to be important for efficient expression of the ribosomal proteins. Furthermore, fusion to ubiquitin increases the yield of cloned gene products in *Escherichia coli* (30). One hypothesis proposed to explain these observations is that ubiquitin may facilitate proper folding or assembly of the fused proteins. The efficiency and speed of the ubiquitin folding reaction *in vitro* is consistent with its potential role as a molecular chaperone.

We thank Michael Sauder for help with experiments and data analysis, Paul Laub for assistance with molecular graphics, and Dr. Gülnur Elöve for advice and discussions. This work was supported by Grants GM44881 and GM35926 from the National Institutes of Health.

1. Kim, P. S. & Baldwin, R. L. (1990) *Annu. Rev. Biochem.* **59**, 631–650.
2. Matthews, C. R. (1991) *Curr. Opin. Struct. Biol.* **1**, 28–35.
3. Roder, H., Elöve, G. A. & Englander, S. W. (1988) *Nature (London)* **335**, 700–704.
4. Udgaonkar, J. B. & Baldwin, R. L. (1988) *Nature (London)* **335**, 694–699.
5. Roder, H. & Wüthrich, K. (1986) *Proteins* **1**, 34–42.
6. Bycroft, M., Matouschek, A., Kellis, J. T., Jr., Serrano, L. & Fersht, A. R. (1990) *Nature (London)* **346**, 488–490.
7. Elöve, G. A. & Roder, H. (1991) *ACS Symp. Ser.* **470**, 50–63.
8. Udgaonkar, J. B. & Baldwin, R. L. (1990) *Proc. Natl. Acad. Sci. USA* **87**, 8197–8201.
9. Kuwajima, K. (1989) *Proteins* **6**, 87–103.
10. Rechsteiner, M., ed. (1988) *Ubiquitin* (Plenum, New York).
11. Monia, B. P., Ecker, D. J. & Crooke, S. T. (1990) *Biotechnology* **8**, 209–215.
12. Vijay-Kumar, S., Bugg, C. E. & Cook, W. J. (1987) *J. Mol. Biol.* **194**, 531–544.
13. DiStefano, D. L. & Wand, A. J. (1987) *Biochemistry* **26**, 7272–7281.
14. Weber, P. L., Brown, S. C. & Mueller, L. (1987) *Biochemistry* **26**, 7282–7290.
15. Pace, C. N. (1986) *Methods Enzymol.* **131**, 266–280.
16. Roder, H. (1989) *Methods Enzymol.* **176**, 446–472.
17. Englander, S. W. & Poulsen, A. (1969) *Biopolymers* **7**, 379–393.
18. Molday, R. S., Englander, S. W. & Kallen, R. G. (1972) *Biochemistry* **11**, 150–158.
19. Roder, H., Wagner, G. & Wüthrich, K. (1985) *Biochemistry* **24**, 7407–7411.
20. Lenkinski, R. E., Chen, D. M., Glickson, J. D. & Goldstein, G. (1977) *Biochim. Biophys. Acta* **494**, 126–130.
21. Tanford, C. (1970) *Adv. Protein Chem.* **24**, 1–95.
22. Quantum Chemistry Program Exchange (1990) PROTEIN ANALYSIS PACKAGE, Program No. 594 (Indiana University, Bloomington, IN).
23. Englander, S. W. & Kallenbach, N. R. (1984) *Quart. Rev. Biophys.* **16**, 521–655.
24. Baldwin, R. L. & Roder, H. (1991) *Curr. Biol.* **1**, 218–220.
25. Nall, B. T. (1985) *Comments Mol. Cell. Biophys.* **3**, 123–143.
26. Grathwohl, C. & Wüthrich, K. (1976) *Biopolymers* **15**, 2025–2046.
27. Levitt, M. (1981) *J. Mol. Biol.* **145**, 251–263.
28. Finley, D., Bartel, B. & Varshavsky, A. (1989) *Nature (London)* **338**, 394–401.
29. Redman, K. L. & Rechsteiner, M. (1989) *Nature (London)* **338**, 438–440.
30. Butt, T. R., Jonnalagadda, S., Monia, B. P., Sternberg, E. J., Marsh, J. A., Stadel, J. M., Ecker, D. J. & Crooke, S. T. (1989) *Proc. Natl. Acad. Sci. USA* **86**, 2540–2544.